Grass Research

ARTICLE

Open Access

https://doi.org/10.48130/grares-0025-0010

Grass Research **2025**, 5: e009

Identification of perennial ryegrass CDPK gene family and function exploration of *LpCDPK27* upon salt stress

Shiyao Chen, Yumiao Xie, Shuyin Pan, Shuhan Yu* and Lu Zhang*

College of Landscape and Architecture, Zhejiang A&F University, Hangzhou 311300, China

* Corresponding authors, E-mail: 20220144@zafu.edu.cn; zhanglu@zafu.edu.cn

Abstract

Calcium serves as a pivotal second messenger in the response to both abiotic and biotic stresses. Calcium-dependent protein kinase (CDPK) plays a significant role in plant development, growth, and adaptation to environmental stresses. In our research, 28 *LpCDPKs* were computationally identified in *Lolium perenne* and divided into Groups I–IV based on phylogenetic relationships. Six genes with promoter regions containing elements related to abiotic stress responsiveness were selected to investigate further whether they were stress-related *LpCDPKs*. The qRT-PCR analysis revealed that most *LpCDPKs* responded to various abiotic stresses and phenotypic validation of overexpressed yeast under stress conditions confirmed these findings. Notably, *LpCDPK27* was strongly induced by salt stress, and its overexpression in Arabidopsis significantly enhanced salt tolerance. *LpCDPK27* overexpressing lines exhibited lower Na^+ content, higher K^+ content, and increased expression of stress-related genes compared to wild-type plants. Collectively, these results provide essential insights into the evolution and function of *LpCDPKs* and offer a valuable resource for future research on the roles of CDPKs in the growth, development, and stress responses of *Lolium perenne*.

Citation: Chen S, Xie Y, Pan S, Yu S, Zhang L. 2025. Identification of perennial ryegrass CDPK gene family and function exploration of *LpCDPK27* upon salt stress. *Grass Research* 5: e009 https://doi.org/10.48130/grares-0025-0010

Introduction

During their growth stages, plants frequently encounter various abiotic and biotic stresses. To cope with these challenges, they have evolved intricate mechanisms and signaling networks that enable them to identify and resist stress, thereby ensuring survival under such conditions[1]. Calcium, serving as an ubiquitous second messenger in eukaryotes, is essential for facilitating plant adaptation to various abiotic and biotic stresses[2]. Diverse stimuli like temperature extremes, water scarcity, high salinity, plant hormones, and pathogens can cause swift and fleeting alterations in the levels of intracellular Ca^{2+} concentration[3]. Those changes are perceived and deciphered by different Ca^{2+}-binding proteins (CBPs) or Ca^{2+} sensors, which then initiate a cascade of downstream reactions[4]. There are five known classes of Ca^{2+} sensors in plants, which include calmodulins (CaMs), calmodulin-like proteins (CMLs), calcium/calmodulin-dependent protein kinase (CCaMK), calcineurin B-like proteins (CBLs), and calcium-dependent protein kinases (CDPKs/CPKs)[5]. The structure of CDPKs is marked by four key conserved domains: an N-terminal domain, a protein kinase domain, an autoinhibitory domain, and a calcium binding domain containing two to four EF-hands[6]. Compared to other Ca^{2+} sensors, CDPKs can directly transmit calcium signals into physiological responses through the phosphorylation of various substrates, including ion channels, transcription factors, and metabolic enzymes, without relying on exogenous calmodulin. This multiplicity of targets that CDPKs interact with bestows upon them essential functions in the regulation of stomatal movements and pollen tube growth, the modulation of hormonal signaling, the orchestration of transcriptional reprogramming, and stress tolerance, which gives CDPKs their dual identities as Ca^{2+} sensors and responders[7,8].

CDPK was first identified in pea (*Pisum sativum*)[9], and subsequent genome-wide screenings have identified CDPKs across a multitude of plant species. Plant genomes like those of *Arabidopsis thaliana*[8], maize (*Zea mays*)[10], rice (*Oryza sativa*)[11], wheat (*Triticum aestivum*)[12], cotton (*Gossypium raimondii*)[13], populus (*Populus trichocarpa*)[14], and *Medicago truncatula*[15], have been shown to harbor 34, 35, 29, 20, 41, 30, and 24 CDPKs, respectively. According to the phylogenetic relationship, expression pattern, and subcellular targeting, all the CDPK gene family members in terrestrial plants are grouped into four subfamilies. Genes within the same subfamily exhibit similar intron-exon structures. Among them, Group IV includes the least number of CDPK gene members[10,11,14,16]. Furthermore, Group IV is more closely related to the CDPK genes of ancient algae than the other three groups.

Previous studies have shown that CDPKs are absent in animals and fungi but exist in plants, protozoa, oomycetes, and green algae[17]. Specific expression of the CDPK genes was detected in various plant tissues, including flower, fruit, root, stem, and leaf. They participate in the modulation of a broad spectrum of physiological processes. For instance, *AtCPK17* and *AtCPK34* have been discovered to have a redundant function in pollen tube growth and significantly influence the efficiency of pollen transfer and the rate of pollen tube growth[18]. *AtCPK28* has regulatory effects on vascular development and stem elongation[19]. Furthermore, CDPKs are also implicated in response to a range of abiotic stresses. *AtCPK8* regulates the activity of CAT3 to control ABA-mediated stomatal movement during drought stress[20]. *OsCPK12* is crucial for salt tolerance and has a positive effect on the detoxification of ROS by regulating the expression of *OsAPx2* and *OsAPx8* to reduce oxidative damage in plant cells at high salinity[21]. The CPK28-NLP7 phosphorylation cascade can decode cold-induced calcium signals rapidly, subsequently enhancing plant cold tolerance[22]. The interaction of *OsCPK17* with sucrose phosphate synthase *OsSPS4*, along with aquaporin *OsPIP2;1/OsPIP2;6*, enhances rice's ability to withstand cold stress[23]. During soybean seed development, GmCDPKSK5 responds to high humidity stress and heat stress by targeting the translationally controlled tumor protein GmTCTP[24]. AtCBK3/AtCPK1

enhances thermotolerance by phosphorylating AtHSFA1a to control the binding activity of heat-shock transcription factor (HSF) DNA to heat-shock element (HSE)[25]. The diverse functionalities of CDPKs allow for their involvement in various stages of plant development. However, little is known about CDPKs in perennial ryegrass.

Perennial ryegrass (*Lolium perenne*) is a kind of cold-season perennial grass that is extensively found in temperate regions globally. It has the advantages of trampling resistance, resistance to diseases and insects, and having a long green period. Nevertheless, the growth and productivity of this grass are constrained by extreme temperatures, drought, and salt stress throughout its life cycle[26]. In particular, the increasing rate of soil salinization in agricultural lands and the growing demand for the use of reclaimed water or other secondary saline sources for turfgrass landscape irrigation have further exacerbated the prevalence of salt stress in turfgrasses[27,28]. To counteract these stresses, plants modulate various physiological, biochemical, and molecular processes via cellular and subcellular signaling pathways. For instance, the mechanisms by which plants adapt to salt stress encompass ion homeostasis, the antioxidant defense system, osmotic adjustment, and hormonal regulation[29]. CDPKs are unique and key calcium-binding proteins that can decrypt and convey calcium signals to activate and regulate various genes, transcription factors, enzymes, and ion channels, thereby modulating tolerance to abiotic stresses[30]. Numerous studies have reported the diverse functions of plant CDPKs in combating salinity stress[7,31–34]. Therefore, this research had a triple aim: firstly, to categorize and analyze the CDPK gene family within perennial ryegrass; secondly, to pinpoint CDPKs that may serve as candidate genes for stress tolerance in this grass species; and thirdly, to identify potential positive regulators of salt stress tolerance.

Materials and methods

Identification and cloning of CDPK family members in *L. perenne*

The full genomic, proteomic, coding sequence (CDS) data, and general feature format (GFF) annotation files of CDPKs were downloaded from the genome databases of *L. perenne* (NCBI, www.ncbi.nlm.nih.gov), *A. thaliana* (TAIR, www.arabidopsis.org), and *O. sativa* (TIGR, http://rice.uga.edu/). The process of identifying potential CDPK genes began with screening for genes with a threshold E-value below 1E-100, both for the complete sequence and the top-performing domain. Further validation of the composition of these potential proteins was carried out using the SMART (http://smart.embl-heidelberg.de) database and the NCBI-conserved domain database (CDD, www.ncbi.nlm.nih.gov/Structure/cdd/wrpsb.cgi). Sequences that contained errors, were shorter than 100 amino acids, or lacked complete Ser/Thr kinase domains (PF00069) and EF-hands domains (PF13499) were not included in the study.

Total mRNA was successfully extracted from *L. perenne* tissues with the aid of the Plant RNA prep pure Kit (Tiangen, China). The Prime Scrip II 1st Strand cDNA Synthesis Kit (TaKaRa, China) was utilized to produce the first-strand cDNA, which was then put to use in gene cloning purposes. Primers targeting the sequences surrounding the open reading frames of all *LpCDPK* genes were used for their cloning. The PCR, conducted in a 50 μL volume, utilized 2 × Phanta Max Master Mix (Vazyme, China) for cloning purposes. The PCR products were purified using a Gel Extraction Kit (Omega Bio-Tek, USA), they were cloned into corresponding modified vectors for sequencing.

Phylogenetic analysis

The construction of the phylogenetic tree involved all CDPKs in *L. perenne* and *A. thaliana* into MEGA 11.0 with the maximum-likelihood method in 1,000 bootstrap replicates by the LG + G + I amino acid substitution model[35]. All the identified *LpCDPKs* were categorized into various groups based on the classification of *AtCPKs* and *OsCDPKs* sequences[8,11]. The final results of the phylogenetic analysis were then visualized by the online tool iTOL (http://itol.embl.de/).

Analysis of characteristics, gene structure, and domain organization

The validated *LpCDPKs* were analyzed using the ExPasy online tool (http://web.expasy.org/protparam/) to compute their physicochemical characteristics, including the molecular weight (MW), theoretical point (pI), and grand average of hydropathicity (GRAVY). The TBtools (Toolbox for Biologists) program was utilized to conduct the examination of the exon-intron composition of *LpCDPK* genes with default parameters. The domain organization was forecasted with the SMART database tool (http://smart.embl-heidelberg.de).

Chromosome locations and synteny correlation analysis

The physical positions on the chromosome of each *LpCDPK* member were ascertained using the genome annotation data. The chromosomal position and the Circos diagram were mapped using TBtools software. To validate and illustrate the syntenic connections between the genes of *L. perenne*, *A. thaliana*, and *O. sativa* homologs, the Multiple Synteny Plot feature within the TBtools was deployed.

Analysis of *cis*-acting regulatory elements

From the genome database of *L. perenne*, the promoter sequence (2,000 bp) upstream from 5'-UTR of all *LpCDPKs* was downloaded. The web-based utility PlantCARE (http://bioinformatics.psb.ugent.be/webtools/plantcare/html/) was then put into action to identify and analyze the *cis*-acting regulatory elements of each gene.

Plant growth conditions and stress treatments

Perennial ryegrass seeds were evenly distributed in a foam container lined with moist paper towels, and subsequently, the container was positioned in a growth chamber of Zhejiang A&F University (Hangzhou, China). Having grown for 7 d, the seedlings were shifted to a hydroponic system using the Hoagland nutrient solution for 2 weeks and kept in a growth chamber set at a day/night temperature cycle of 26/20 °C, a light/dark period of 14/10 h, and a photosynthetically active radiation (PAR) was maintained at 750 μmol photos $m^{-2}{\cdot}s^{-1}$, and a relative humidity of 70%. The Hoagland nutrient solution was refreshed in the hydroponic container every 3 d to ensure the plants received sufficient oxygen and nutrients.

To determine *LpCDPKs* expression patterns under stress, plants were subjected to heat (38 °C), cold (4 °C), high salt stress (255 mM), and osmotic stress (15% PEG6000, w/v). For RNA extraction, samples of leaves and roots were harvested at intervals of 0, 2, 6, 8, 12, and 24 h after each stress treatment.

Analysis of quantitative real-time polymerase chain reaction

We carried out quantitative real-time polymerase chain reaction (qRT-PCR) analysis following the protocol outlined in a previous investigation[36]. The specific primers employed in the qRT-PCR are outlined in Supplementary Table S1, *LpeIHF4A* and *AtACTIN2* were chosen as the reference genes[37,38].

Stress tolerance studies in yeast

Six *LpCDPK* genes (*LpCDPK5*, *LpCDPK7*, *LpCDPK10*, *LpCDPK15*, *LpCDPK20,* and *LpCDPK27*) that had elements related to abiotic stress-responsiveness in promoter regions were selected, to identify

LpCDPKs involved in stress responses. The corresponding coding sequences (CDS) corresponding to those *LpCDPKs* were generated by using gene-specific primers detailed in Supplementary Table S2 and introduced into the pYES2 vector. Then, those constructed vectors and empty pYES2 (control) plasmids were transformed into the yeast strain INVSc1 through the use of Chemically Competent Cell (Weidibio, Shanghai, China). The transformants were selected by their growth on the SC/-Ura medium containing glucose (SD/-Ura) at 28 °C. Positive colonies were identified using the Yeast Colony PCR kit (Weidibio, Shanghai, China). For the stress assay, the positive colonies were cultured in SD/-Ura medium at 28 °C in a shaking table overnight at OD600 = 0.6–0.8. After washing those samples 3–5 times in SC/-Ura medium, the yeast cell densities were adjusted to OD600 = 0.6, and then cultured on SC/-Ura medium containing galactose (SG/-Ura) at 28 °C for 24 h to promote gene expression. At the end of incubation, 50 μL (OD600 = 1.0) of yeast cell culture solutions was removed, using sterile water to dilute these samples by 10-fold (10^0, 10^{-1}, 10^{-2}, 10^{-3}, and 10^{-4}). Then, 8 μL of the cell solution was spread onto the surface of the solidified SG/-Ura medium. For the drought and salt stress treatments, 800 mM mannitol, and 500 mM NaCl were added to the medium respectively, and the plates were incubated in an incubator at 28 °C together with the control group. For the heat stress and cold stress treatment groups, the medium was incubated at 37 and 20 °C respectively.

Analysis of subcellular localization

The terminal stop codon was omitted when amplifying the CDS of the selected *LpCDPKs* using gene-specific primers listed in Supplementary Table S3. These sequences were then inserted into the pCAMBIA1305-GFP vector to form *LpCDPK*-GFP fusion genes, which were subsequently delivered into the *Agrobacterium tumefaciens* strain 'EHA105'. *Agrobacterium tumefaciens* was cultured overnight at OD600 = 1.0, then it was resuspended with an infective solution at OD600 = 0.6, and this solution was used to infiltrate the leaves of *Nicotiana benthamiana* aged 4–6 weeks. Following infiltration, the leaves were kept in the dark for 12 h before being returned to standard growth conditions. The GFP fluorescence was examined on the third day by employing the Zeiss LSM 800 laser scanning confocal microscope from Carl Zeiss SAS in Jena, Germany.

Generation of transgenic plants

The CDS of *LpCDPK27* was successfully cloned into the pCAMBIA3301 binary vector. Subsequently, the recombinant vector was introduced into *Arabidopsis thaliana* ecotype Columbia via *Agrobacterium tumefaciens*-mediated floral dip transformation. The progeny was screened on 1/2 MS medium with the Basta to select for transgenic plants. Homozygous T_3 generation transgenic seeds were harvested and subsequently utilized for further research.

Analysis of salt tolerance

Arabidopsis seeds were disinfected by soaking in an 8% (v/v) sodium hypochlorite solution for 12 min and then thoroughly rinsed with sterile water three times. A total of 50 disinfected seeds were placed on 1/2 MS medium supplemented with 0, 75, or 100 mM NaCl. The seeded plates were subjected to a 4 °C cold treatment in a fridge for 2 d before being transferred to a growth chamber set at 25 °C with 16-h light and 8-h dark photoperiod to assess germination rates. To determine the amount of taproot elongation, seeds that had germinated on the 1/2 MS medium were transplanted onto fresh square plates containing 0, 75, 100, or 125 mM NaCl and placed in a 25 °C light culture chamber for vertical growth for 14 d.

Seven-day-old Arabidopsis seedlings, initially cultivated on 1/2 MS medium, were transplanted into soil and grown in a greenhouse at 25 °C for 3 weeks to assess salt tolerance at the rosette stage. For survival rate determination, potted plants were given 200, 250, and 300 mM NaCl solutions for 5 d each, followed by 350 mM NaCl solutions for 7 d, and finally with water for 2 weeks to leach the salt from the soil. Meanwhile, those irrigated completely with water throughout the trial were used as controls. The survival rate was calculated by counting the surviving plants. Excluding the measurement of survival rate, the electrolyte leakage (EL) was measured 5 d after salt treatment using a conductivity meter (LEICI DDS-11A) following the procedure described in the internal control. In these experiments, each measurement was conducted with a minimum of three replicates.

Determination of sodium and potassium ions in leaves

The contents of sodium (Na^+) and potassium (K^+) in the plants were measured using a previously reported method[39]. Plants that were 3 weeks of age and soil-grown were irrigated with a 75 mM NaCl solution to facilitate the uptake of Na^+ and K^+. After 10 d of salt treatment, the aerial parts of the plants were collected, rinsed with deionized water, and then placed in an oven to dry until their weight stabilized. The dehydrated plant material was ground into a powder, and 0.1 g of sample was added to 6 mL of 65% (v/v) nitric acid. The samples were digested in a microwave at 170 °C for 40 min. After the extracts were diluted with ddH_2O to a final volume of 30 mL, the contents of Na^+ and K^+ were measured with inductively coupled plasma optical emission spectrometry (ICP-OES, Optima 8000; Perkinelmer, USA).

Statistical analysis

Prism 10.0 software was utilized to analyze the data, which were presented as means ± standard deviation (n = 3). One-way or two-way ANOVA was conducted to confirm the significance of the differential expression.

Results

Identification of 28 CDPK family members in *L. perenne*

A total of 28 *LpCDPKs* were identified based on *L. perenne* genome sequences using SMART and CDD software. Depending on their chromosomal positions, they were denominated as *LpCDPK1* to *LpCDPK28*. The features of the genes under study were further detailed, including several key parameters such as their gene locus identifiers, gene and protein, pI, MW, GRAVY, and number of EF-hand motifs (Supplementary Table S4). The CDS lengths of *LpCDPKs* ranged from 1,161 bp (*LpCDPK6*) to 3,603 bp (*LpCDPK26*), averaging 1,719 bp. The encoded protein length ranged from 386 (LpCDPK6) to 1,200 (LpCDPK26) amino acids (aa), with an average of 572 aa. While the pI varied from 4.95 (*LpCDPK22*) to 9.52 (*LpCDPK3*), and the average value was 6.17. The MW varied from 43.52 (*LpCDPK6*) to 130.18 kDa (*LpCDPK26*), with an average of 63.33 kDa. The grand average of GRAVY values for the *LpCDPKs* spanned from −0.516 for *LpCDPK11* to −0.221 for *LpCDPK10*, suggesting that these *LpCDPK* proteins are hydrophilic. Furthermore, it was anticipated that each *LpCDPK* would contain between two to four EF-hand motifs within their CaM-like domain, enabling the capability to recognize and bind calcium Ca^{2+} molecules[40].

Phylogenetic relationships of *LpCDPKs*

To determine the evolutionary connections among the LpCDPK proteins, a comprehensive alignment was conducted using TBtools software, which included all CDPK members from *L. perenne* (28). *A. thaliana* (34), *O. sativa* (29). This alignment resulted in the

generation of an unrooted phylogenetic tree as depicted in Fig. 1. The CDS and corresponding protein sequences of LpCDPK are listed in Supplementary Tables S5 and S6. CDPK proteins in *L. perenne* were divided into four groups (Groups I–IV). Group I comprised 11 LpCDPKs, followed by Group II and Group III, which comprised eight and seven, respectively, while the remaining two proteins were placed in Group IV. The majority of the LpCDPKs were found in Group I and Group II, which exhibited similarities to the AtCPK and OsCDPK proteins. In addition, most *LpCDPKs* presented highly conserved motifs with other plants' CDPKs, such as *AtCDPKs* or *OsCDPKs*.

Domain architectures and gene structure

Almost all members of the CDPK family have four conserved domains, namely the N-terminal variable domain (V), the protein kinase domain (K), the auto-inhibitory domain (I), and the calcium-binding domain (C) conceived with one to four EF-hands (Fig. 2b). Four conserved EF-hands were present in most *LpCDPK* members (21), six members (*LpCDPK04*, *LpCDPK06*, *LpCDPK11*, *LpCDPK20*, *LpCDPK25,* and *LpCDPK26*) contained three EF-hands while only *LpCDPK03* has one EF-hand. In particular, *LpCDPK26* also has two zinc-binding motifs in addition to four EF-hands.

The structural analysis of *LpCDPKs* was conducted by examining the pattern of exon/intron organization. There was considerable variation in gene structure among the *LpCDPKs*, with differences in both the number and length of introns, except for some homologous genes that showed similar structures. Each gene possesses a long initial exon, succeeded by a series of shorter exons that range from 1 to 11 in total (Fig. 2c). The intron phase for all *LpCDPK* gene models was also assessed. As shown in Fig. 2c, all *LpCDPKs* have phase 0, 1, or 2.

Chromosomal location and synteny analysis of *LpCDPK* genes

TBtools software was employed to examine the chromosomal location of *LpCDPKs,* revealing that these genes are scattered across eight chromosomes with non-uniform distribution patterns and densities (Fig. 3). The maximal number of *LpCDPKs* (25%) was found on chromosome 4. Gene collinearity among *LpCDPKs* was explored through duplication analysis, uncovering a total of six pairs of duplicated genes (Fig. 3). BLASTp and MCScanX (Multiple Collinear Scan Toolkit) were used for the analysis of duplication patterns (tandem and segment repeats). It was found that six pairs of *LpCDPKs* were paralogous and belonged to segmented duplication. No instances of tandem duplication were detected in this study. The data imply that segmental duplication was a key factor in the evolutionary process of *LpCDPKs*. Moreover, the orthologous relationship between 28 *LpCDPK* genes and 34 *AtCPK* genes from Arabidopsis as well as 29 *OsCDPK* genes from rice, was investigated. The analysis indicated the presence of three pairs of orthologous CDPKs between *L. perenne* and *A. thaliana* and 40 pairs between *L. perenne* and *O. sativa* (Fig. 4). With TBtools software, calculations were performed for the synonymous substitution rate (Ks) and the non-synonymous substitution rate (Ka) of the gene pairs to verify the presence of effective selection pressure. All those gene pairs exhibited Ka/Ks values below 0.3 (Supplementary Table S7), suggesting that there was a strong purification selection in those gene pairs.

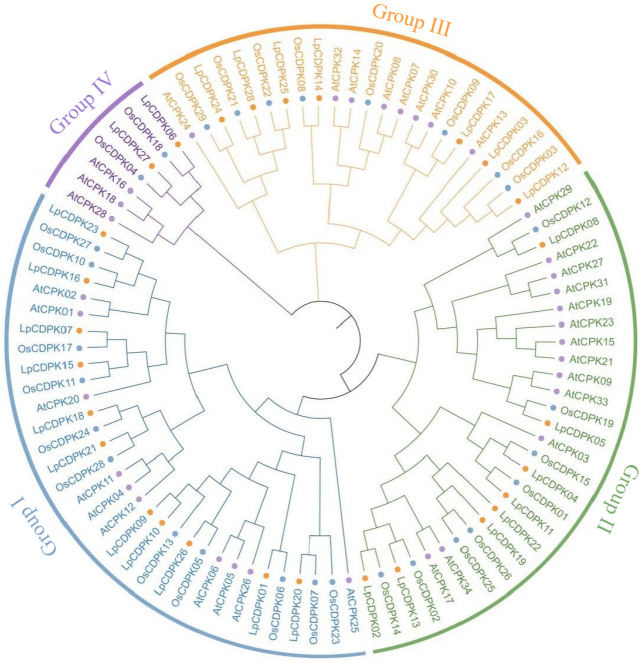

Fig. 1 Phylogenetic tree of *CDPK* proteins in *L. perenne* (orange circle), *A. thaliana* (purple circle), and *O. sativa* (blue circle). Different colors represent different groups of *LpCDPK*.

Analysis of *cis*-acting elements in the promoter region of *LpCDPKs*

To understand the regulatory mechanisms and possible functions of the *LpCDPK* genes in plant development and stress responses, we used PlantCARE to examine the *cis*-acting elements within a 2.0 kb DNA sequence of the promoter region. The *LpCDPKs* possess promoter regions that are rich in *cis*-acting elements concerning stress, phytohormonal influence, growth, and developmental stages. While there is significant variation in the distribution of these elements across the CDPK promoters (Fig. 5a), all of the CDPKs contain hormone-responsive elements. Three hundred and thirty one stress and phytohormone-responsive *cis*-acting elements were detected across all *LpCDPK* genes (Fig. 5b; Supplementary Table S8), including 124 Methyl Jasmonate responsive elements, 89 ABA response elements, 26 drought-responsive elements, 26 auxin-responsive elements, 23 gibberellin responsive elements, 19 low-temperature responsive elements, 13 salicylic acid-responsive elements, six circadian control responsive elements, four defense and stress-responsive elements, and one wound-responsive element. Those results indicated that *LpCDPKs* may play potential roles in the regulation of multiple responses to environmental stress, phytohormones, and development.

Relative expression levels of *LpCDPKs* in roots and leaves under abiotic stress

Investigating the *cis*-acting elements within the promoter region may offer circumstantial support for deciphering the functions of CDPK genes in response to stress[41]. To identify potential abiotic stress-responsive candidate *LpCDPKs*, six *LpCDPKs* (*LpCDPK5*, *LpCDPK7*, *LpCDPK10 LpCDPK15, LpCDPK20,* and *LpCDPK27*) that had elements related to abiotic stress-responsiveness in promoter regions were chosen for qRT-PCR analysis under four abiotic stresses (heat, cold, osmotic, and salt stress) at five-time points. The findings revealed that the selected *LpCDPK* genes exhibited distinct expression patterns in response to various stresses, suggesting their involvement in the regulatory mechanisms of abiotic stress responses (Fig. 6; Supplementary Table S9).

The heat and cold treatments led to upregulation of the expression of these *LpCDPKs*, and in most cases, the transcriptional responses of five *LpCDPKs* (except for *LpCDPK7*) to heat or cold treatments showed greater intensity in roots compared to leaves (Fig. 6a–d). For instance, *LpCDPK15* expression was enhanced 5- to 23-fold in roots, yet the increase in leaves was below 6-fold. Under

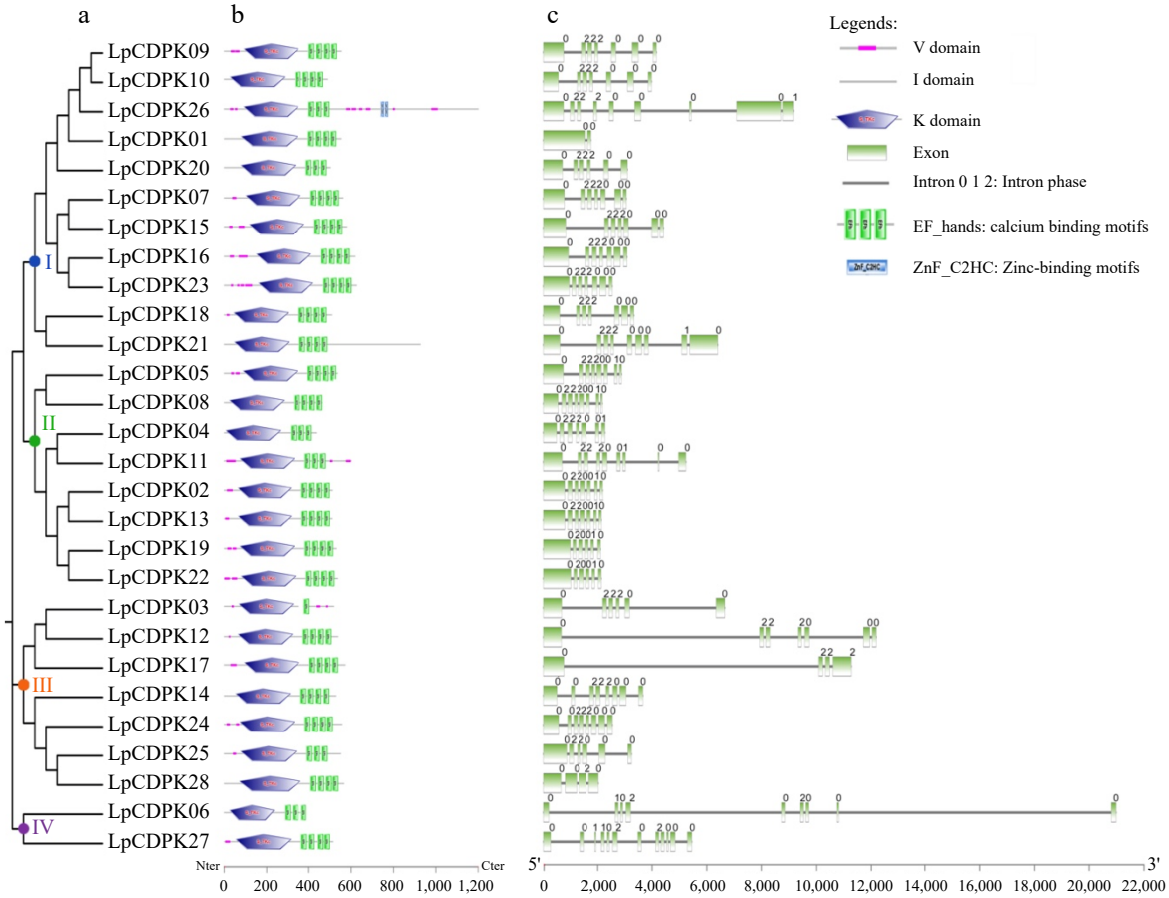

Fig. 2 Analyses of the evolutionary ties, domain architecture, and exon-intron pattern of CDPK family members in *L. perenne*. (a) An unrooted phylogenetic tree illustrating the *LpCDPKs* is drawn using the maximum-likelihood method in MEGA 11.0. (b) The domain architecture of *LpCDPKs* is presented. Visual representations of these domains were sourced from the EMBL-EBI and SMART online tools and modified using Adobe Photoshop CS6. (c) The exon/intron pattern of CDPK family genes in *L. perenne* is detailed, with the numbers 0, 1, and 2 denoting the intron phase within the sequence.

osmotic treatment (Fig. 6e, f), three of the *LpCDPKs* were downregulated in the root, including *LpCDPK5*, *LpCDPK7*, and *LpCDPK15*, but in leaves, the expression of *LpCDPK5* and *LpCDPK7* was upregulated. *LpCDPK10* was also a gene whose expression levels in roots and leaves had opposite response trends, the expression of *LpCDPK10* in roots showed an upward trend, while that in leaves showed a downward trend. In addition, the transcriptional response of *LpCDPK27* maintained obvious expression in both roots and leaves. Except for *LpCDPK27* which was only induced by salt, and *LpCDPK7* which was only repressed by salt, the four others exhibited both repression and induction to various levels in roots (Fig. 6g). In leaves, *LpCDPK10* and *LpCDPK15* remained at low levels in all periods after salt treatment, and the expression levels of the rest of the *LpCDPKs* increased by 3 to 10-fold, respectively (Fig. 6h).

Comparison of yeast growth under salt and drought stress

To identify *LpCDPKs* involved in abiotic stress, six genes were expressed in the INVSC1 yeast strain. Transgenic yeast cells of six *LpCDPK* genes and *pYES2* control grew well and were not different from the control (Fig. 7). When subjected to heat or salt stress, the transgenic yeast strains harboring *pYES2-LpCDPK5/7/10/20/27* exhibited enhanced growth compared to the control. This suggests that these *LpCDPKs* may contribute to heat and salt tolerance. Similarly, under cold or drought stress, the strains with *pYES2-LpCDPK10/20/27* also showed improved growth, indicating their potential involvement in cold and drought tolerance. These results collectively suggest that the overexpression of certain *LpCDPK* genes can enhance the stress tolerance of yeast cells under various abiotic stress conditions, including heat, cold, salt, and drought.

Subcellular localization of LpCDPK protein

CDPKs show widespread subcellular distribution, which is one of the reasons they can participate in various physiological processes in different cellular compartments. Therefore, we performed transient expression of selected LpCDPKs-GFP in tobacco leaves to determine their functional cellular compartments. The results indicated that LpCDPK5 and LpCDPK10 were co-localized with nucleus-marker OsMADS, and plasma membrane (PM) marker AtAKT1 after plasmolysis, indicating that they were detected on the nuclei and plasma membrane. Besides, LpCDPK7, LpCDPK15, LpCDPK20, and LpCDPK27 were co-localized with PM.marker AtAKT1 after plasmolysis (Fig. 8), indicating that those four genes were only detected on the plasma membrane.

Overexpression of *LpCDPK27* confers enhanced salt tolerance in Arabidopsis

In relative expression levels analysis, *LpCDPK27* was the highest induced by salt stress treatment, suggesting a possible part it plays in controlling salt tolerance. To delve into the function of *LpCDPK27* under salt stress, three representative transgenic lines (OE4, OE5, and OE8) with the highest expression of *LpCDPK27* were selected according to qRT-PCR for salt tolerance evaluation (Supplementary Fig. S1). As depicted in Fig. 9a, b, the seed germination rate reached 97% in 2 d, and both wild-type (WT) and transgenic lines exhibited equivalent behavior under control conditions. Both 75 and 100 mM

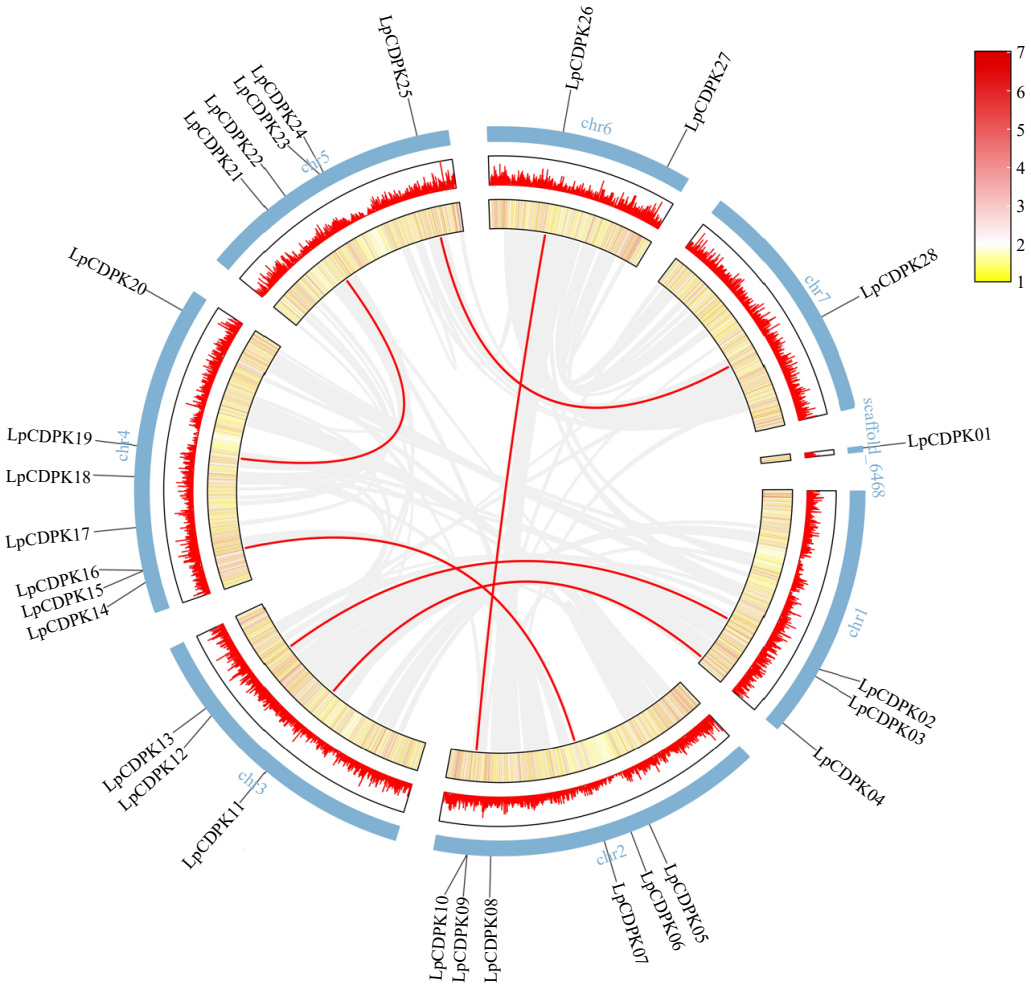

Fig. 3 Chromosomal locations and synteny analysis of *LpCDPK* genes. Red lines indicate duplicate gene pairs. The density of genes on chromosomes is represented by the heatmap (the yellow ring and the red ring).

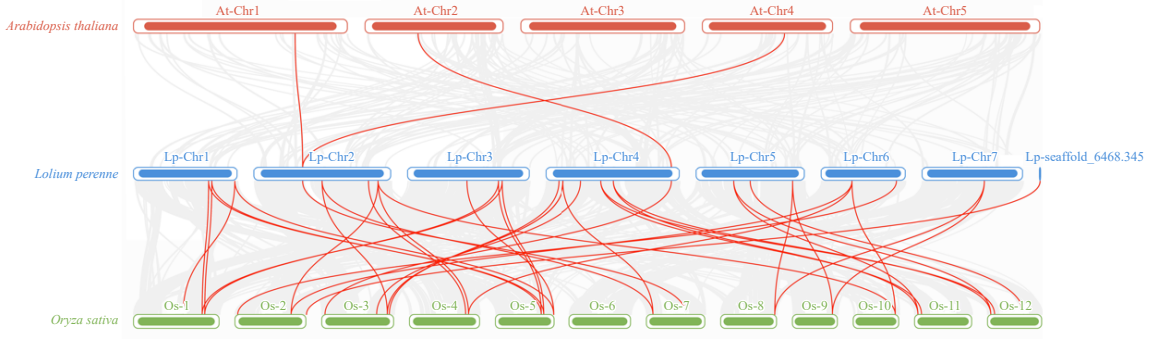

Fig. 4 The analysis of synteny among *LpCDPK* genes in the genomes between *L. perenne* and *A. thaliana* or *O. sativa*. The red lines indicate the syntenic gene pairs between *L. perenne* and *A. thaliana* or *O. sativa*, with chromosome numbers displayed above each chromosome.

NaCl decreased the germination rate of all plants, whereas the transgenic lines were seen to have a higher germination rate than those in WT (Fig. 9c, d). The salt tolerance of seedlings was assessed according to the root length which revealed no growth difference under control conditions between the WT and transgenic types. However, when subjected to 75, 100, and 125 mM NaCl, the growth of both genotypes was stunted, characterized by smaller frames and shorter roots, yet the transgenic plants displayed greater root elongation than the WT (Fig. 10a, b). The capacity to tolerate salt at the rosette stage was additionally tested by irrigating 3-week-old soil-grown plants with a NaCl solution to assess EL and survival rate. The transgenic varieties displayed superior survival rates in contrast to the WT, and they also presented with lower EL levels (Fig. 10c–e). This data illustrated that an excess of *LpCDPK27* expression in transgenic Arabidopsis contributes to increased salt tolerance.

To explore if the expression of *LpCDPK27* regulated ion homeostasis, The determination of Na^+ and K^+ levels in the shoots was conducted following 75 mM NaCl treatment so as not to damage the plant by ion. There was no significant difference of Na^+ and K^+ in shoots between the two genotypes under the control condition (Fig. 11a). However, after salt treatment, the concentration of Na^+ increased significantly and K^+ decreased, the transgenic lines exhibited lower Na^+ and higher K^+ concentrations compared to the WT (Fig. 11b). These alterations led to increased Na^+/K^+ ratios in all

Fig. 5 Investigating the *cis*-acting elements within the *LpCDPK* gene promoters. (a) Identifying the location of the promoter *cis*-element, (b) assessing the quantity of these elements within the *LpCDPK* promoter regions, with the annotations of their functions provided on the left side of the corresponding image.

plants, but the ratios were lower in the transgenic plants as compared to the WT (Fig. 11c). Moreover, the expression levels of SOS pathway genes (SOS1, SOS2, and SOS3) and potassium transporter gene AKT2 were compared between *LpCDPK27*-OE lines and WT, both with and without NaCl treatment. After salt treatment, transgenic lines showed an increase in SOS1, SOS2, SOS3, and AKT2 transcript levels compared to the WT (Fig. 11d–g). These findings indicated that *LpCDPK27* expression modulated the expression of genes related to ion homeostasis and stress response, contributing to enhanced salt tolerance in the transgenic plants.

Discussion

CDPK genes are prevalent across the plant kingdom and function in regulating numerous physiological processes and plant development[17]. The advent of advanced whole-genome sequencing has facilitated the exploration of the genomic identification and evolutionary relationships of the CDPK family in multiple species. In this work, 28 CDPK genes have been identified in *L. perenne,* which were designated as *LpCDPK1-LpCDPK28* in accordance with the proposed nomenclature for CDPK genes[42]. Phylogenetic analysis revealed that *LpCDPKs* were akin to those of other species, clustering into four groups with comparable numbers of Group III and Group IV genes, yet differing in the count of Group I and Group II genes when compared to other plants. This finding suggests that the variation in CDPK gene numbers across species is largely due to the independent evolution of Group I or Group II genes[43]. Featuring a conserved kinase domain, CDPKs are equipped with an auto-inhibitory segment that links to a calmodulin-like domain responsible for Ca^{2+} binding. Such structural attributes enable CDPKs to interpret fluctuations in cytoplasmic Ca^{2+} levels, prompted by hormonal signals and various biotic and abiotic stressors[44]. The conservation and variation in CDPK gene structures underpin the expansion of this gene family and the conservation or diversification of their functions. Structural characteristics like active sites, acylation sites, and exon-intron structures, reveal details

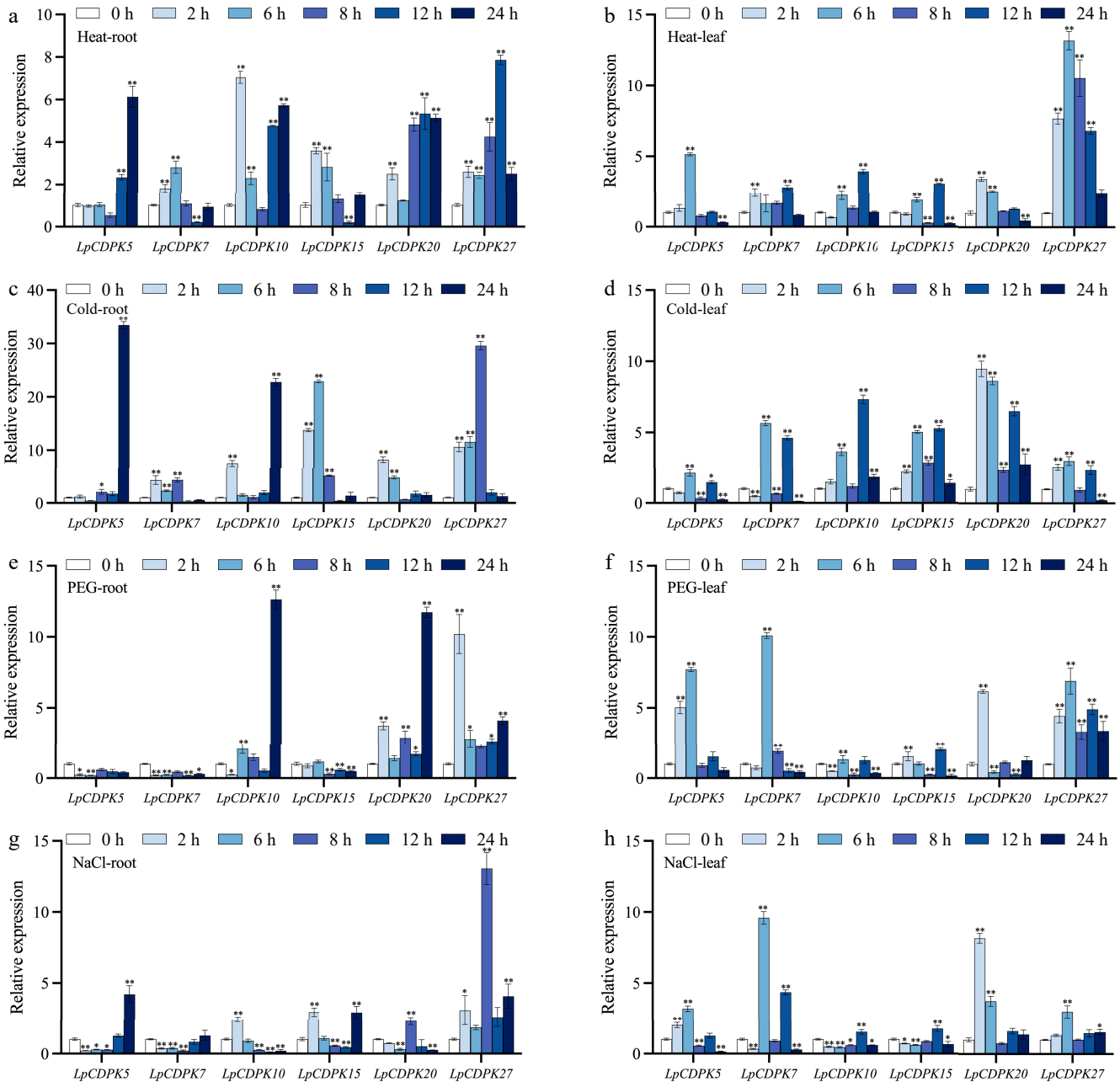

Fig. 6 The expression patterns of *LpCDPKs* in both roots and leaves of perennial ryegrass were examined under a variety of abiotic stress conditions. (a), (b) Exposure to high temperature stress at 38 °C; (c), (d) subjected to cold stress at 4 °C; (e), (f) challenged with osmotic stress with 15% PEG 6000; (g), (h) treated with salt stress at a concentration of 255 mM. Values are depicted as mean values coupled with their standard deviations (n = 3). The relative expression levels of the *LpCDPK* genes were determined using the $2^{-\Delta\Delta C_T}$ method. * $p < 0.05$, ** $p < 0.01$.

about the evolution and divergence of gene families. Introns are crucial for growth, development, and evolutionary processes[45]. Analysis of gene structure indicated that the majority of *LpCDPK* genes contained five or six introns, but *LpCDPK27* had 10 introns. Only *LpCDPK1* did not contain introns, while *LpCDPK17* and *LpCDPK28* had two introns. We speculated that the low intron numbers were due to the loss of introns during the evolution of perennial ryegrass[46,47]. Paralogs with a similar intron phase are believed to share a common ancestor, and shifts in intron phase signify divergence of paralogs over vast periods, potentially up to a billion years[48]. By analyzing the intron phase for *LpCDPKs*, we observed that all of them possessed phases 0, 1, or 2, a record of significant evolutionary milestones. It was also found that exon-intron organization patterns and intron phase were similar among members of the same CDPK gene subfamily across both the perennial ryegrass genome and other plant species, indicating that an origin for the CDPK genes is the same among different plants and they are closely evolutionarily conserved. Those results strongly endorse the close evolutionary relationships of *LpCDPKs* and the categorization into Groups I–IV.

Plant evolution is largely driven by gene duplication, which results in the proliferation of gene families. Various models of gene duplication exist, including segmental, tandem, proximal, dispersed, and transposed duplication[49]. Those duplicate processes can result in functional redundancy, neo-functionalization, and sub-functionalization[50]. In this study, we found six duplication events in the *L. perenne* genome, *LpCDPK02*/*LpCDPK13*, *LpCDPK04*/*LpCDPK11*, *LpCDPK07*/*LpCDPK15*, *LpCDPK09*/*LpCDPK26*, *LpCDPK19*/

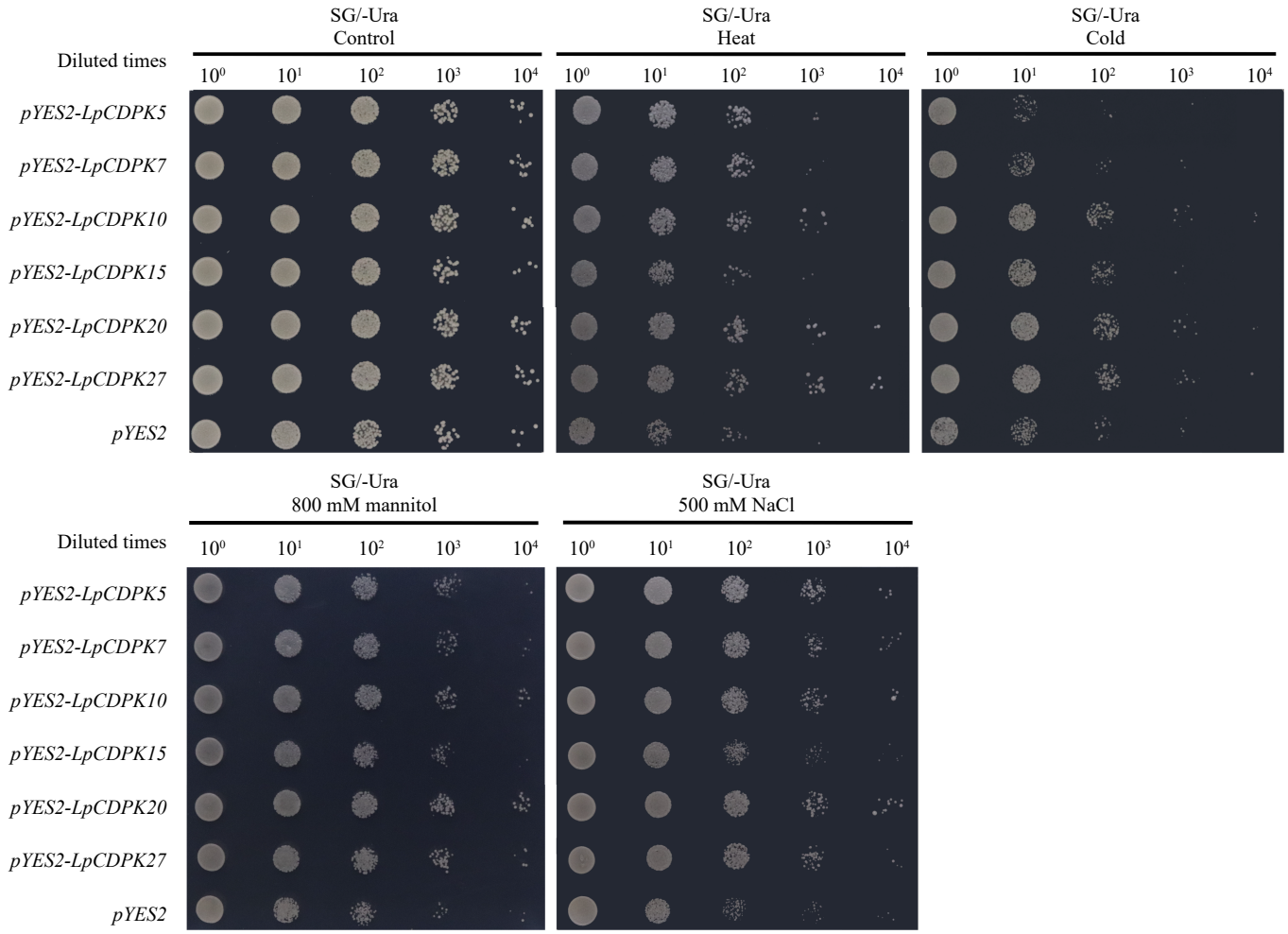

Fig. 7 Heat, cold, drought, and salt stress tolerance of *LpCDPK5*, *LpCDPK7*, *LpCDPK10*, *LpCDPK15*, *LpCDPK20*, and *LpCDPK27* in a yeast expression system, using yeast with an empty *pYES2* vector as a control.

LpCDPK22, and *LpCDPK25*/*LpCDPK28*, all of which were segmental duplications. This finding indicated that the expansion of the CDPK gene in *L. perenne* was due to segmental duplication events. To determine the selective pressure acting on these duplicated genes, we evaluated the non-synonymous to synonymous substitution ratio (Ka/Ks) for each duplicated CDPK gene pair. Generally, a Ka/Ks value above 1 signifies positive selection, a value of 1 indicates neutral selection and a value below 1 denotes purifying or negative selection[51]. For six pairs of duplicated CDPK genes, the Ka/Ks ratios were all below 0.243, indicating that these pairs had primarily undergone strong purifying selection pressure following segmental duplications and may cause limited function divergence.

In our research, we investigated the possible impact of the *LpCDPK* gene on responses to abiotic stress. For the precise regulation of gene expression across space, time, and within specific cells, the regulatory elements in the promoter region are of paramount importance[52]. All six selected genes that had elements associated with abiotic stress-responsiveness in the promoter region showed reactions to various abiotic stresses, and this was also corroborated by phenotypic validation in yeast stress resistance assays. However, no MYB binding site for drought-inducible element (MBS) was found on promoters of *LpCDPK5*, and no low-temperature stress response element (LTRE) was found on promoters of *LpCDPK10*, *LpCDPK15*, *LpCDPK20*, and *LpCDPK27*, even though these genes show responsiveness to drought or cold stress. On the contrary, although *LpCDPK15* did contain the MBS, it had no significant response to drought stress according to the experimental results of qRT-PCR analysis and phenotypic verification of yeast stress resistance (Figs 6 & 7). Similar results were also found in *Gossypium Raimondii*[43], *Melilotus albus*[53], and *Solanum habrochaites*[51]. These findings suggested that there may be other, yet unidentified, stress-related *cis*- or *post*-transcriptional regulatory mechanisms involved in the regulation of *LpCDPK*.

Myristic and palmitic acylation are unique in lipid modifications[54]. Myristoylation (irreversible) has been shown to promote membrane association of *LeCPK1*[55], *OsCPK2*[56], and *AtCPK2*[57]. The S-acyl group (palmitoyl moiety) itself has been demonstrated to confer a membrane affinity approximately tenfold stronger than that of a single N-myristoyl group[58]. Myristoylation on its own is usually not enough for membrane localization, and it needs to cooperate with palmitoylation to permanently anchor proteins on membranes to promote proteins to perform physiological functions[59,60]. All six of the genes we selected had palmitoylation sites, and except for *LpCDPK10* and *LpCDPK15*, the other four genes also had N-myristoylation sites. Subcellular location analysis showed that *LpCDPK5* and *LpCDPK10* were detected on the nuclei and plasma membrane. While *LpCDPK7*, *LpCDPK15*, *LpCDPK20*, and *LpCDPK27* were only detected on the plasma membrane. These results were similar to those of their orthologous genes, which also have the N-terminal acylation site[60]. In addition, palmitoylation aids in modulating cellular activities, including hormone signaling, disease resistance, and stress response[58]. Moreover, palmitoylation

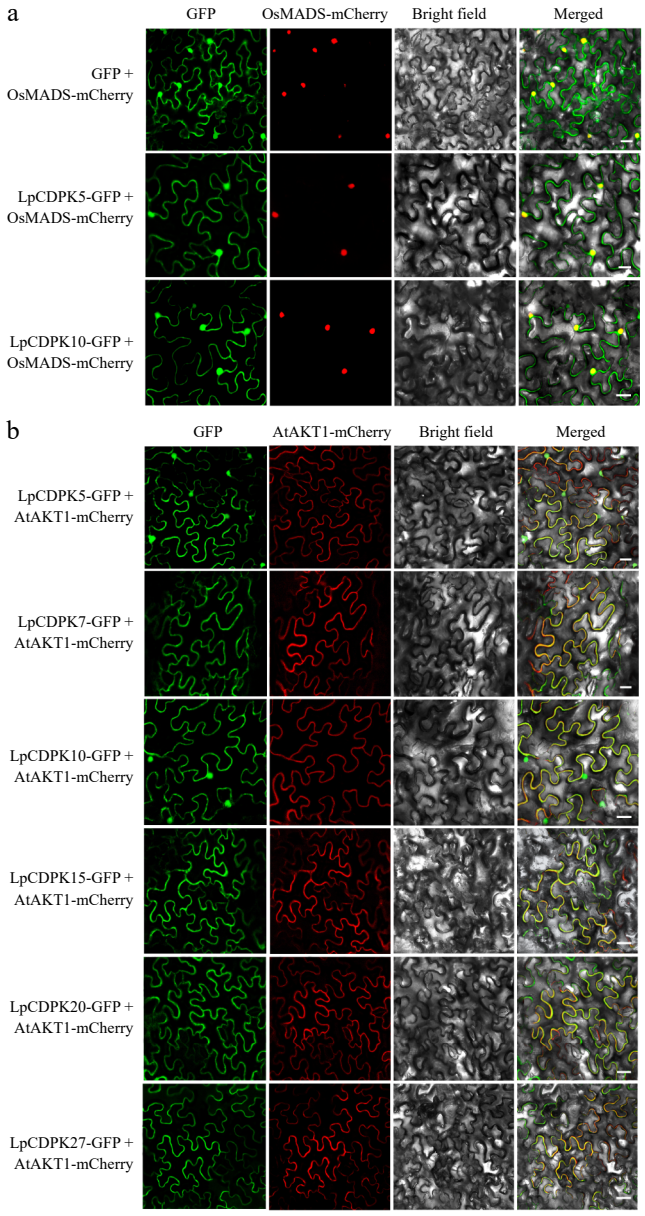

Fig. 8 Subcellular localization of LpCDPKs. The injected tobacco was used for observation. The vector pCAMBIA1305 was used as the control. The nucleus-marker: (a) nucleus localization protein OsMADS, and PM-marker: (b) plasma membrane localization protein AtAKT1 were used, respectively. Bars = 20 μm.

is reversible, enabling the detachment of membrane-bound proteins to be released from the membrane through thioesterase-catalyzed de-palmitoylation and subsequently translocated to the cytosol or nucleus[61]. It has been reported that the subcellular locations of *AtCPK10*, *AtCPK30*, and *AtCPK32* moved from the plasma membrane to the nucleus when exposed to nitrate[62]. Such shifts in subcellular localization offer CDPKs the potential to engage in diverse physiological functions. This study lays the groundwork for further investigation into the roles of *LpCDPKs* in *L. perenne*.

The balance of Na^+ and K^+ in cells is pivotal for plant salt tolerance, with diverse mechanisms employed by different plant species to sustain this ion balance[63]. Under salt treatment, the *LpCDPK27*-OE lines exhibited reduced Na^+ levels, elevated K^+ levels, and consequently, significantly lower Na^+/K^+ ratios compared to the WT (Fig. 11), indicating that *LpCPDK27* expression modulated the homeostasis of Na^+ and K^+. The SOS pathway is recognized as a significant regulatory mechanism for ion homeostasis, enhancing the sodium tolerance in plants under salt stress[64]. Elevated salinity triggers calcium signaling, sensed by SOS3, leading to the subsequent activation of SOS2. Activated SOS2 then phosphorylates SOS1, boosting its transport activity. This leads to SOS1 pumping out excess Na^+ from cells, thus lowering intracellular Na^+ levels[64,65]. AKT2, a member of the Shaker family of K^+ channels, is crucial for the transport of K^+ in and out of phloem tissues[66]. These regulatory pathways are essential for maintaining Na^+/K^+ homeostasis in *Arabidopsis thaliana* when subjected to salt stress. In this study, SOS1, SOS2, SOS3, and AKT2 transcripts were induced in transgenic lines following salt treatment, whereas no significant changes were observed in the WT plants. This correlated with the observed reduction in Na^+ levels and increase in K^+ levels in the transgenic lines under salt tolerance conditions. The findings suggested that the improved Na^+ and K^+ balance attributed to *LpCDPK27* expression was linked to the increased expression of SOS1, SOS2, SOS3, and AKT2 under saline conditions. *LpCDPKs* are a class of enzymes that can directly translate calcium signals into physiological responses. They regulate a variety of physiological processes through the phosphorylation of downstream target proteins. Under salt stress conditions, the concentration of calcium ions within plant cells undergoes changes. Once these changes are sensed by *LpCDPKs*, their kinase activity is activated, leading to the phosphorylation of downstream target proteins, thereby modulating the plant's salt tolerance. *LpCDPK27* may exert its regulatory effects on the balance of Na^+ and K^+ within cells by phosphorylating Na^+/K^+ transporters, thereby influencing their activity and endogenous levels. However, we have not yet experimentally validated the specific mechanisms of action for *LpCDPK27*. Based on existing literature and related studies, we speculate that *LpCDPK27* may regulate the salt stress response through the following mechanisms: (1) Phosphorylation of Na^+/K^+ transporters: *LpCDPK27* may phosphorylate Na^+/K^+ transporters such as SOS1 and AKT2, thereby modulating their activities. SOS1 is a key protein in plant salt tolerance, responsible for extruding Na^+ from the cell to lower intracellular Na^+ concentrations[64]. AKT2 is involved in the uptake and transport of K^+, maintaining intracellular K^+ levels[67]. The overexpression of *LpCDPK27* may enhance the activities of these transporters through phosphorylation, thereby improving plant salt tolerance. (2) Regulation of the SOS signaling pathway: The SOS signaling pathway is a crucial regulatory pathway for plant salt tolerance. *LpCDPK27* may modulate the activities of SOS2 or SOS3 through phosphorylation, thereby enhancing the activity of SOS1. SOS2 is a protein kinase that phosphorylates SOS1 to activate its Na^+ extrusion function[68–70]. SOS3 is a calcium-binding protein that senses intracellular calcium signals and activates SOS2[71]. *LpCDPK27* may enhance the perception and response to calcium signals by phosphorylating SOS2 or SOS3, thereby improving plant salt tolerance[70].

The identification and functional exploration of *LpCDPK* genes in perennial ryegrass revealed that several members of this family, particularly *LpCDPK20* and *LpCDPK27*, exhibit significant responses to various abiotic stresses, suggesting their potential roles in stress tolerance mechanisms. Overall, whether in the qRT-PCR or the yeast expression system, *LpCDPK20* and *LpCDPK27* remained highly expressed in all four biological stresses. And the subcellular localization of them on the plasma membrane suggests that it may directly interact with external stress signals and regulate downstream signaling pathways through phosphorylation of membrane-associated proteins. These results collectively highlight the potential roles of *LpCDPK20* and *LpCDPK27* in stress tolerance mechanisms in perennial ryegrass. Furthermore, OsCDPK7 and AtCPK6, the orthologous to *LpCDPK20*, were verified to be positive regulators and showed

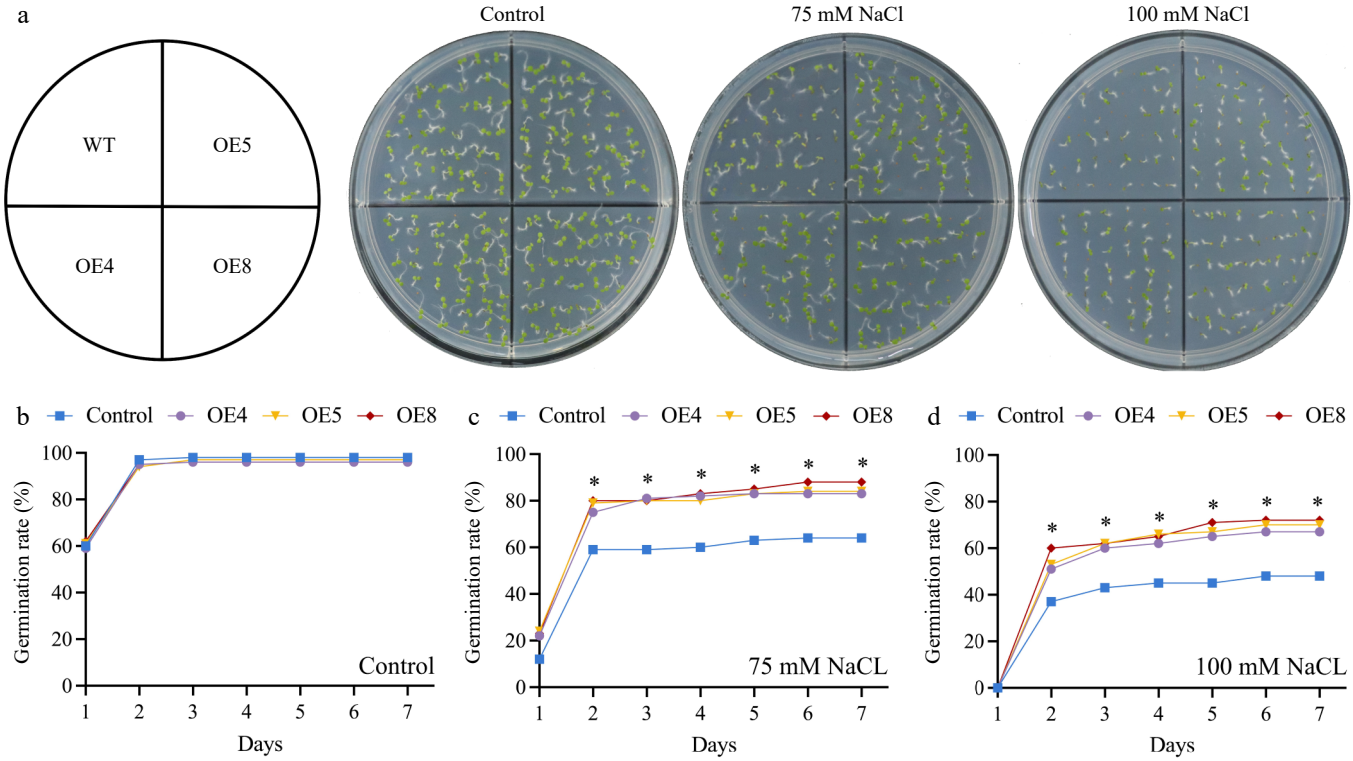

Fig. 9 Assessing the impact of *LpCDPK27* overexpressing Arabidopsis on seed germination under saline conditions involved comparing these lines to wild-type controls. (a) Photos were captured after a 7-d germination period on 1/2 MS medium supplemented with either 0, 75, or 100 mM NaCl. The germination rates on 1/2 MS medium with (b) 0, (c) 75, and (d) 100 mM NaCl were examined. Values are depicted as mean values coupled with their standard deviations (n = 3, with 50 seeds per replicate). * denotes a statistically significant difference between the transgenic and wild-type lines for the specified time point ($p < 0.05$).

transcriptional activation to high salinity stress, drought, and/or cold[33,72]. Given the conservation of gene functions in plants during evolution, *LpCDPK20* is likely to inherit similar functions and play an important positive regulatory role in perennial ryegrass responding to abiotic stress. However, a notable distinction emerged when examining their expression patterns more closely. *LpCDPK27* displayed the most substantial overall increase in expression levels across all four abiotic stresses in qRT-PCR analyses. This comprehensive and pronounced upregulation under diverse stress conditions suggests that *LpCDPK27* may play a particularly crucial and broad-spectrum role in the stress response mechanisms of perennial ryegrass. While our primary focus has been on the salt tolerance function of *LpCDPK27*, we have also observed significant upregulation of *LpCDPK27* under heat stress conditions. In fact, in an unpublished study, we have detailed the role of *LpCDPK27* in enhancing heat tolerance in perennial ryegrass. Our findings indicate that *LpCDPK27* not only contributes to salt tolerance but also plays a crucial role in heat stress responses. This dual functionality highlights the broad-spectrum stress tolerance potential of *LpCDPK27* and underscores the importance of further exploring its molecular mechanisms in different stress contexts. While *LpCDPK27* has been the primary focus of our current functional studies, the significant stress-responsive expression of *LpCDPK20*, along with its demonstrated ability to enhance stress tolerance in yeast, indicates that it is also a promising candidate for future research. The distinct expression patterns of *LpCDPK20* and *LpCDPK27* highlight the complexity and diversity of the CDPK gene family in stress responses. It is likely that different *LpCDPK* genes may have specialized roles in responding to specific stress conditions or may act synergistically to enhance overall stress tolerance in perennial ryegrass. Therefore, our future research will continue to explore the functions of *LpCDPK20* and other stress-responsive *LpCDPK* genes. A comprehensive investigation of the entire CDPK gene family in perennial ryegrass will provide a more holistic understanding of their roles in stress tolerance and may reveal additional valuable genetic resources for improving the resilience of this important turfgrass species to adverse environmental conditions. Additionally, further elucidation of the molecular mechanisms underlying the dual roles of *LpCDPK27* in salt and heat tolerance will contribute to a more comprehensive understanding of the stress response network in perennial ryegrass.

Conclusions

In our research, 28 *CDPKs* in perennial ryegrass were determined and characterized. The *LpCDPKs* had conservative and divergence structures that facilitated the growth of gene family and the conservation or differentiation of functions, while they were under strong purifying selection pressure after segmental duplication and were highly homologous to *OsCDPKs*. Moreover, according to qRT-PCR analysis and the yeast ectopic expression system, most of the selected *LpCDPKs* had shown sensitivity to various non-biological stressors, and *LpCDPK20* and *LpCDPK27* were screened as candidate genes for stress resilience. Furthermore, the regulation of salt tolerance by *LpCDPK27* in Arabidopsis was positively correlated with the preservation of Na^+ and K^+ ion balance during saline conditions, due to the induced expression of SOS1, SOS2, SOS3, and AKT2. The findings from our study will facilitate further functional dissection of the *LpCDPK* gene family and can inform molecular breeding strategies for perennial ryegrass.

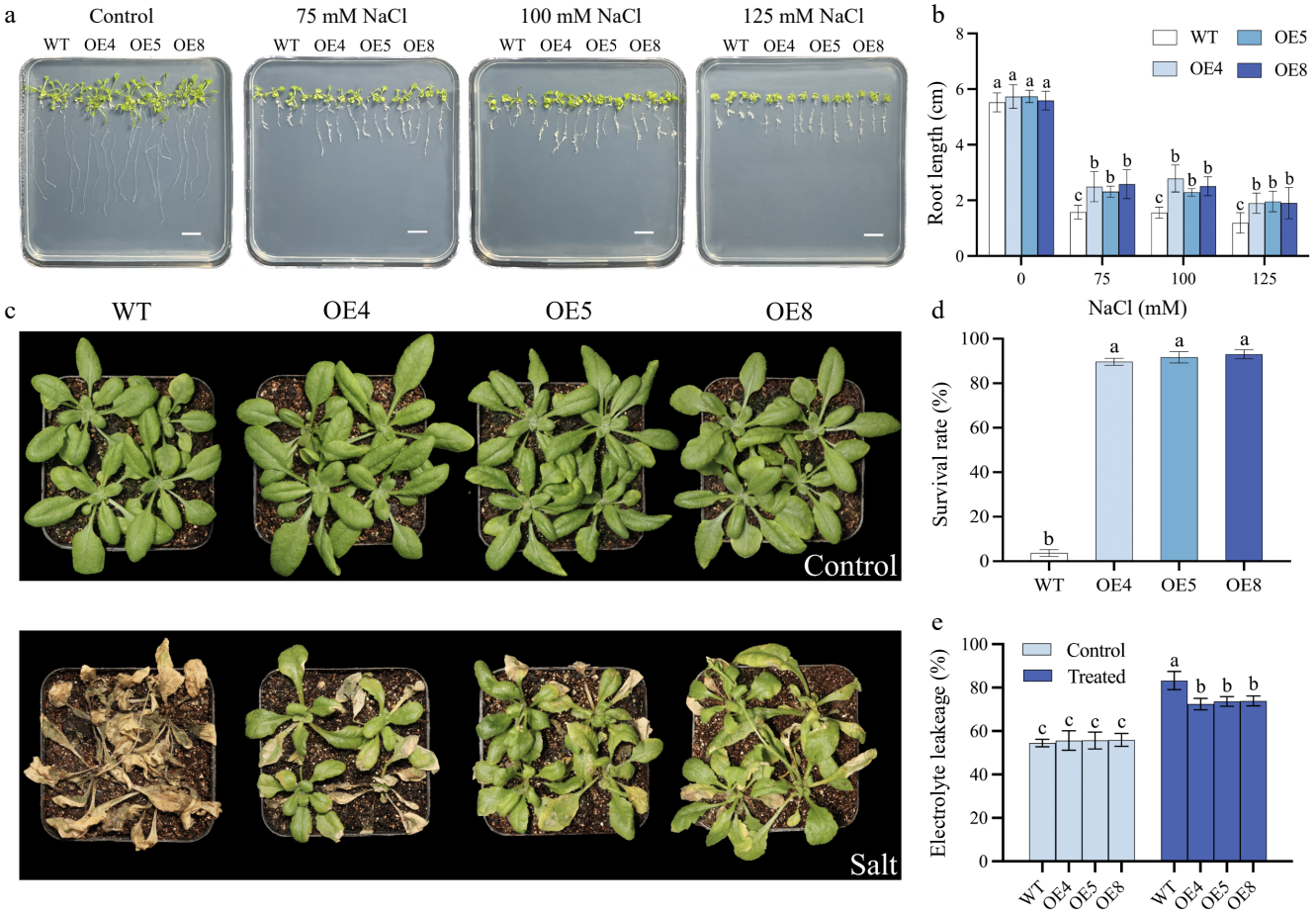

Fig. 10 Salt tolerance assessment of Arabidopsis over-expressed of *LpCDPK27*. (a) Germinated seeds were grown on 1/2 MS medium with varying NaCl concentrations of 0, 75, 100, or 125 mM. Images were captured after 14 d of growth (scale bars = 10 mm), (b) after which the length of the primary roots is determined. (c) The appearance of transgenic and wild-type Arabidopsis at 4 weeks of age, with or without NaCl treatment for 22 d, is documented following a 2-week salt removal period through watering. (d) The survival rates are figured out by comparing the count of surviving plants to the total number of plants. (e) Electrolyte leakage is assessed 5 d post-salt treatment. Data presented are the mean and standard deviation (n = 3, with four replicate pots per treatment). A common letter superimposed on the bars signifies no significant difference at the $p > 0.05$ level.

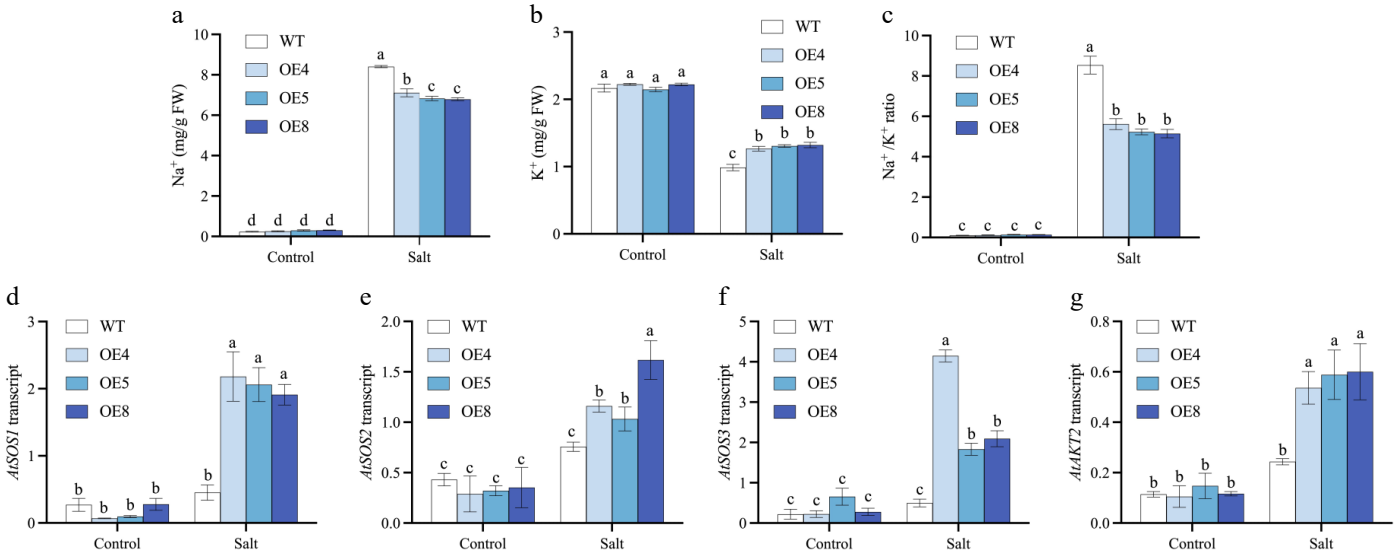

Fig. 11 Investigations are conducted on the levels of Na^+ and K^+, as well as the relative expression levels of genes related to ion homeostasis and stress responsiveness, in *LpCDPK27* overexpressing Arabidopsis lines vs wild-type plants following exposure to saline conditions. Three-week-old seedlings are subjected to 75 mM NaCl for 10 d, after which the shoots were collected for (a) Na^+ and (b) K^+ level measurements. (c) The Na^+/K^+ ratio is derived from these measurements. Following a 6-h treatment with 50 mM NaCl, total RNA extraction is performed from leaf tissues. The transcript levels of (d) SOS1, (e) SOS2, (f) SOS3, and (g) AKT2 are subsequently quantified using qRT-PCR. Values are depicted as mean values coupled with their standard deviations (n = 3). A common letter superimposed on the bars signifies no significant difference at the $p > 0.05$ level.

Author contributions

The authors confirm contribution to the paper as follows: writing - original draft, investigation, visualization, data curation: Chen S; investigation: Xie Y, Pan S; methodology, funding acquisition, writing - review & editing: Yu S; funding acquisition, writing - review & editing, supervision: Zhang L. All authors reviewed the results and approved the final version of the manuscript.

Data availability

All data generated or analyzed during this study are included in this published article and its supplementary information files.

Acknowledgments

This work was funded by the National Natural Science Foundation of China (32171687 and 32211530421), and the Personnel Startup Project of the Scientific Research and Development Foundation of Zhejiang A&F University (2021FR041 and 2023LFR039).

Conflict of interest

The authors declare that they have no conflict of interest.

Supplementary information accompanies this paper at (https://www.maxapress.com/article/doi/10.48130/grares-0025-0010)

Dates

Received 18 January 2025; Revised 16 February 2025; Accepted 26 February 2025; Published online 17 March 2025

References

1. Zhu JK. 2016. Abiotic stress signaling and responses in plants. *Cell* 167:313–24
2. Mohanta TK, Bashir T, Hashem A, Abd-Allah EF, Khan AL, et al. 2018. Early events in plant abiotic stress signaling: Interplay between calcium, reactive oxygen species and phytohormones. *Journal of Plant Growth Regulation* 37:1033–49
3. Lee HJ, Seo PJ. 2021. Ca^{2+} talyzing initial responses to environmental stresses. *Trends in Plant Science* 26:849–70
4. Kudla J, Becker D, Grill E, Hedrich R, Hippler M, et al. 2018. Advances and current challenges in calcium signaling. *New Phytologist* 218:414–31
5. Ketehouli T, Quoc VHN, Dong J, Do H, Li X, et al. 2022. Overview of the roles of calcium sensors in plants' response to osmotic stress signalling. *Functional Plant Biology* 49:589–99
6. Bredow M, Monaghan J. 2022. Cross-kingdom regulation of calcium- and/or calmodulin-dependent protein kinases by phospho-switches that relieve autoinhibition. *Current Opinion in Plant Biology* 68:102251
7. Shi S, Li S, Asim M, Mao J, Xu D, et al. 2018. The *Arabidopsis* calcium-dependent protein kinases (CDPKs) and their roles in plant growth regulation and abiotic stress responses. *Journal of Experimental Botany* 19:1900
8. Yip Delormel T, Boudsocq M. 2019. Properties and functions of calcium-dependent protein kinases and their relatives in *Arabidopsis thaliana*. *New Phytologist* 224:585–604
9. Hetherington A, Trewavas A. 1982. Calcium-dependent protein kinase in pea shoot membranes. *FEBS Letters* 145:67–71
10. Kong X, Lv W, Jiang S, Zhang D, Cai G, et al. 2013. Genome-wide identification and expression analysis of calcium-dependent protein kinase in maize. *BMC Genomics* 14:433
11. Asano T, Tanaka N, Yang G, Hayashi N, Komatsu S. 2005. Genome-wide identification of the rice calcium-dependent protein kinase and its closely related kinase gene families: comprehensive analysis of the *CDPKs* gene family in rice. *Plant and Cell Physiology* 46:356–66
12. Hu CH, Li BB, Chen P, Shen HY, Xi WG, et al. 2023. Identification of CDPKs involved in *TaNOX7* mediated ROS production in wheat. *Frontiers in Plant Science* 13:1108622
13. Gao W, Xu FC, Guo DD, Zhao JR, Liu J, et al. 2018. Calcium-dependent protein kinases in cotton: insights into early plant responses to salt stress. *BMC Plant Biology* 18:15
14. Zuo R, Hu R, Chai G, Xu M, Qi G, et al. 2013. Genome-wide identification, classification, and expression analysis of CDPK and its closely related gene families in poplar (*Populus trichocarpa*). *Molecular Biology Reports* 40:2645–62
15. Zhao P, Liu Y, Kong W, Ji J, Cai T, et al. 2021. Genome-wide identification and characterization of calcium-dependent protein kinase (CDPK) and CDPK-related kinase (CRK) gene families in *Medicago truncatula*. *International Journal of Molecular Sciences* 22:1044
16. Li AL, Zhu YF, Tan XM, Wang B, Wei B, et al. 2008. Evolutionary and functional study of the CDPK gene family in wheat (*Triticum aestivum* L.). *Plant Molecular Biology* 66:429–43
17. Valmonte GR, Arthur K, Higgins CM, MacDiarmid RM. 2014. Calcium-dependent protein kinases in plants: evolution, expression and function. *Plant and Cell Physiology* 55:551–69
18. Myers C, Romanowsky SM, Barron YD, Garg S, Azuse CL, et al. 2009. Calcium-dependent protein kinases regulate polarized tip growth in pollen tubes. *The Plant Journal* 59:528–39
19. Matschi S, Werner S, Schulze WX, Legen J, Hilger HH, et al. 2013. Function of calcium-dependent protein kinase CPK28 of *Arabidopsis thaliana* in plant stem elongation and vascular development. *The Plant Journal* 73:883–96
20. Zou JJ, Li XD, Ratnasekera D, Wang C, Liu WX, et al. 2015. Arabidopsis CALCIUM-DEPENDENT PROTEIN KINASE 8 and CATALASE3 function in abscisic acid-mediated signaling and H_2O_2 homeostasis in stomatal guard cells under drought stress. *The Plant Cell* 27:1445–60
21. Asano T, Hayashi N, Kikuchi S, Ohsugi R. 2012. CDPK-mediated abiotic stress signaling. *Plant Signaling & Behavior* 7:817–21
22. Ding Y, Yang H, Wu S, Fu D, Li M, Gong Z, et al. 2022. CPK28-NLP7 module integrates cold-induced Ca^{2+} signal and transcriptional reprogramming in *Arabidopsis*. *Science Advances* 8:7901
23. Almadanim MC, Alexandre BM, Rosa MTG, Sapeta H, Leitão AE, et al. 2017. Rice calcium-dependent protein kinase *OsCPK17* targets plasma membrane intrinsic protein and sucrose-phosphate synthase and is required for a proper cold stress response. *Plant, Cell & Environment* 40:1197–213
24. Wang S, Tao Y, Zhou Y, Niu J, Shu Y, et al. 2017. Translationally controlled tumor protein GmTCTP interacts with GmCDPKSK5 in response to high temperature and humidity stress during soybean seed development. *Plant Growth Regulation* 82:187–200
25. Liu H, Gao F, Li G, Han J, Liu D, et al. 2008. The calmodulin-binding protein kinase 3 is part of heat-shock signal transduction in *Arabidopsis thaliana*. *The Plant Journal* 55:760–73
26. Miao C, Zhang Y, Bai X, Qin T. 2022. Insights into the response of perennial ryegrass to abiotic stress: underlying survival strategies and adaptation mechanisms. *Life* 12:860
27. Sun S, An M, Han L, Yin S. 2015. Foliar application of 24-epibrassinolide improved salt stress tolerance of perennial ryegrass. *HortScience* 50:1518–23
28. Wu W, Zhang Q, Ervin EH, Yang Z, Zhang X. 2017. Physiological mechanism of enhancing salt stress tolerance of perennial ryegrass by 24-epibrassinolide. *Frontiers in Plant Science* 8:1017
29. Zhao C, Zhang H, Song C, Zhu JK, Shabala S. 2020. Mechanisms of plant responses and adaptation to soil salinity. *The Innovation* 1:100017
30. Atif RM, Shahid L, Waqas M, Ali B, Rashid MAR, et al. 2019. Insights on calcium-dependent protein kinases (CPKs) signaling for abiotic stress tolerance in plants. *International Journal of Molecular Sciences* 20:5298
31. Mehlmer N, Wurzinger B, Stael S, Hofmann-Rodrigues D, Csaszar E, et al. 2010. The Ca^{2+}-dependent protein kinase CPK3 is required for MAPK-independent salt-stress acclimation in Arabidopsis. *The Plant Journal* 63:484–98
32. Mori IC, Murata Y, Yang Y, Munemasa S, Wang YF, et al. 2006. CDPKs CPK6 and CPK3 function in ABA regulation of guard cell S-type anion- and Ca^{2+}-permeable channels and stomatal closure. *PLoS Biology* 4:e327

33. Xu J, Tian YS, Peng RH, Xiong AS, Zhu B, et al. 2010. *AtCPK6*, a functionally redundant and positive regulator involved in salt/drought stress tolerance in Arabidopsis. *Planta* 231:1251–60
34. Zhao R, Sun H, Zhao N, Jing X, Shen X, et al. 2015. The *Arabidopsis* Ca^{2+}-dependent protein kinase *CPK27* is required for plant response to salt-stress. *Gene* 563:203–14
35. Yu S, Sun Q, Wu J, Zhao P, Sun Y, et al. 2021. Genome-wide identification and characterization of short-chain dehydrogenase/reductase (SDR) gene family in *Medicago truncatula*. *International Journal of Molecular Sciences* 22:9498
36. Zhang J, Yu G, Wen W, Ma X, Xu B, et al. 2016. Functional characterization and hormonal regulation of the pheophytinase gene *LpPPH* controlling leaf senescence in perennial ryegrass. *Journal of Experimental Botany* 67:935–45
37. Huang L, Yan H, Jiang X, Yin G, Zhang X, et al. 2014. Identification of candidate reference genes in perennial ryegrass for quantitative RT-PCR under various abiotic stress conditions. *PLoS ONE* 9:e93724
38. Zhang H, Li X, Yu D, Guan J, Ding H, et al. 2023. A vector-free gene interference system using delaminated Mg-Al-lactate layered double hydroxide nanosheets as molecular carriers to intact plant cells. *Plant Methods* 19(1):44
39. Dai M, Huang R, Han Y, Zhang Z, Chen Y, et al. 2022. A novel salt responsive *PvHAK16* negatively regulates salt tolerance in transgenic *Arabidopsis thaliana*. *Environmental and Experimental Botany* 194:104689
40. Mohanta TK, Yadav D, Khan AL, Hashem A, Abd-Allah EF, et al. 2019. Molecular players of EF-hand containing calcium signaling event in plants. *International Journal of Molecular Sciences* 20:1476
41. Yu TF, Zhao WY, Fu JD, Liu YW, Chen M, et al. 2018. Genome-wide analysis of CDPK family in *Foxtail Millet* and determination of *SiCDPK24* functions in drought stress. *Frontiers in Plant Science* 9:651
42. Cheng SH, Willmann MR, Chen HC, Sheen J. 2002. Calcium signaling through protein kinases. The Arabidopsis calcium-dependent protein kinase gene family. *Plant Physiology* 129:469–85
43. Liu W, Li W, He Q, Daud MK, Chen J, et al. 2014. Genome-wide survey and expression analysis of calcium-dependent protein kinase in *Gossypium raimondii*. *PLoS ONE* 9:e98189
44. Alves HLS, Matiolli CC, Soares RC, Cecília Almadanim M, Margarida Oliveira M, et al. 2021. Carbon/nitrogen metabolism and stress response networks - calcium-dependent protein kinases as the missing link? *Journal of Experimental Botany* 72:4190–201
45. Rose AB. 2008. Intron-mediated regulation of gene expression. In *Nuclear pre-mRNA Processing in Plants*, eds Reddy ASN, Golovkin M. Heidelberg: Springer. Vol 326. pp. 277–90. doi: 10.1007/978-3-540-76776-3_15
46. Parvathaneni RK, DeLeo VL, Spiekerman JJ, Chakraborty D, Devos KM. 2017. Parallel loss of introns in the *ABCB1* gene in angiosperms. *BMC Evolutionary Biology* 17:238
47. Yan H, Jiang C, Li X, Sheng L, Dong Q, et al. 2014. PIGD: a database for intronless genes in the Poaceae. *BMC Genomics* 15:832
48. Li L, Yu D, Zhao F, Pang C, Song M, et al. 2015. Genome-wide analysis of the calcium-dependent protein kinase gene family in *Gossypium raimondii*. *Journal of Integrative Agriculture* 14:29–41
49. Qiao X, Li Q, Yin H, Qi K, Li L, et al. 2019. Gene duplication and evolution in recurring polyploidization–diploidization cycles in plants. *Genome Biology* 20:38
50. Liu C, Zhang TZ. 2019. Functional diversifications of *GhERF1* duplicate genes after the formation of allotetraploid cotton. *Journal of Integrative Plant Biology* 61:60–74
51. Li Y, Zhang H, Liang S, Chen X, Liu J, et al. 2022. Identification of *CDPK* gene family in *Solanum habrochaites* and its function analysis under stress. *International Journal of Molecular Sciences* 23:4227
52. Li IMH, Liu K, Neal A, Clegg PD, De Val S, et al. 2018. Differential tissue specific, temporal and spatial expression patterns of the Aggrecan gene is modulated by independent enhancer elements. *Scientific Reports* 8:950
53. Wang S, Duan Z, Yan Q, Wu F, Zhou P, et al. 2022. Genome-wide identification of the GRAS family genes in *Melilotus albus* and expression analysis under various tissues and abiotic stresses. *International Journal of Molecular Sciences* 23:7403
54. Hemsley PA. 2015. The importance of lipid modified proteins in plants. *New Phytologist* 205:476–89
55. Rutschmann F, Stalder U, Piotrowski M, Oecking C, Schaller A. 2002. *LeCPK1*, a calcium-dependent protein kinase from tomato. Plasma membrane targeting and biochemical characterization. *Plant Physiology* 129:156–68
56. Martín ML, Busconi L. 2000. Membrane localization of a rice calcium-dependent protein kinase (CDPK) is mediated by myristoylation and palmitoylation. *The Plant Journal* 24:429–35
57. Lu SX, Hrabak EM. 2002. An *Arabidopsis* calcium-dependent protein kinase is associated with the endoplasmic reticulum. *Plant Physiology* 128:1008–21
58. Hemsley PA, Grierson CS. 2008. Multiple roles for protein palmitoylation in plants. *Trends in Plant Science* 13:295–302
59. Kwiatkowska K, Matveichuk OV, Fronk J, Ciesielska A. 2020. Flotillins: at the intersection of protein S-palmitoylation and lipid-mediated signaling. *International Journal of Molecular Sciences* 21:2283
60. Simeunovic A, Mair A, Wurzinger B, Teige M. 2016. Know where your clients are: subcellular localization and targets of calcium-dependent protein kinases. *Journal of Experimental Botany* 67:3855–72
61. Duan M, Zhang R, Zhu F, Zhang Z, Gou L, et al. 2017. A lipid-anchored NAC transcription factor is translocated into the nucleus and activates glyoxalase I expression during drought stress. *The Plant Cell* 29:1748–72
62. Liu K, Niu Y, Konishi M, Wu Y, Du H, et al. 2017. Discovery of nitrate–CPK–NLP signalling in central nutrient-growth networks. *Nature* 545:311–16
63. Hussain S, Hussain S, Ali B, Ren X, Chen X, et al. 2021. Recent progress in understanding salinity tolerance in plants: story of Na^+/K^+ balance and beyond. *Plant Physiology and Biochemistry* 160:239–56
64. Wang Y, Pan C, Chen Q, Xie Q, Gao Y, et al. 2023. Architecture and autoinhibitory mechanism of the plasma membrane Na^+/H^+ antiporter SOS1 in *Arabidopsis*. *Nature Communications* 14:4487
65. Yang Y, Guo Y. 2018. Unraveling salt stress signaling in plants. *Journal of Integrative Plant Biology* 60:796–804
66. Sandmann M, Skłodowski K, Gajdanowicz P, Michard E, Rocha M, et al. 2011. The K^+ battery-regulating *Arabidopsis* K^+ channel AKT2 is under the control of multiple post-translational steps. *Plant Signaling & Behavior* 6:558–62
67. Chérel I, Michard E, Platet N, Mouline K, Alcon C, et al. 2002. Physical and functional interaction of the Arabidopsis K^+ channel AKT2 and phosphatase AtPP2CA. *The Plant Cell* 14:1133–46
68. Liu J, Ishitani M, Halfter U, Kim CS, Zhu JK. 2000. The *Arabidopsis thaliana SOS2* gene encodes a protein kinase that is required for salt tolerance. *Proceedings of the National Academy of Sciences of the United States of America* 97:3730–74
69. Quintero FJ, Ohta M, Shi H, Zhu JK, Pardo JM. 2002. Reconstitution in yeast of the *Arabidopsis* SOS signaling pathway for Na^+ homeostasis. *Proceedings of the National Academy of Sciences of the United States of America* 99:9061–66
70. Gong Z, Xiong L, Shi H, Yang S, Herrera-Estrella LR, et al. 2020. Plant abiotic stress response and nutrient use efficiency. *Science China Life Sciences* 63:635–74
71. Liu J, Zhu JK. 1998. A calcium sensor homolog required for plant salt tolerance. *Science* 280:1943–45
72. Saijo Y, Hata S, Kyozuka J, Shimamoto K, Izui K. 2000. Over-expression of a single Ca^{2+}-dependent protein kinase confers both cold and salt/drought tolerance on rice plants. *The Plant Journal* 23:319–27